



HAL
open science

Evaluation of aerosol chemical speciation monitor response to different mixtures of organic and inorganic aerosols

Luminița Mărmureanu, Cristina Antonia Marin, Jeni Vasilescu, Jean-Eudes Petit, Tanguy Amodeo, Francois Truong, Bogdan Antonescu, Maria Cruz Minguillon, David Green, Bibi Zainab, et al.

► To cite this version:

Luminița Mărmureanu, Cristina Antonia Marin, Jeni Vasilescu, Jean-Eudes Petit, Tanguy Amodeo, et al.. Evaluation of aerosol chemical speciation monitor response to different mixtures of organic and inorganic aerosols. *Aerosol Science and Technology*, 2024, pp.1-18. 10.1080/02786826.2024.2412999 . hal-04781085

HAL Id: hal-04781085

<https://hal.science/hal-04781085v1>

Submitted on 14 Nov 2024

HAL is a multi-disciplinary open access archive for the deposit and dissemination of scientific research documents, whether they are published or not. The documents may come from teaching and research institutions in France or abroad, or from public or private research centers.

L'archive ouverte pluridisciplinaire **HAL**, est destinée au dépôt et à la diffusion de documents scientifiques de niveau recherche, publiés ou non, émanant des établissements d'enseignement et de recherche français ou étrangers, des laboratoires publics ou privés.



Distributed under a Creative Commons Attribution 4.0 International License



Evaluation of aerosol chemical speciation monitor response to different mixtures of organic and inorganic aerosols

Luminița Mărmureanu, Cristina Antonia Marin, Jeni Vasilescu, Jean-Eudes Petit, Tanguy Amodeo, Francois Truong, Bogdan Antonescu, Maria Cruz Minguillon, David C. Green, Bibi Zainab, Jurgita Ovadnevaite, Thomas Elste, Esther Coz, James Allan, Philip L. Croteau, John Jayne, Manjula R. Canagaratna, Leah Williams, Valerie Gros, Andre S. H. Prevot, Olivier Favez & Evelyn Freney

To cite this article: Luminița Mărmureanu, Cristina Antonia Marin, Jeni Vasilescu, Jean-Eudes Petit, Tanguy Amodeo, Francois Truong, Bogdan Antonescu, Maria Cruz Minguillon, David C. Green, Bibi Zainab, Jurgita Ovadnevaite, Thomas Elste, Esther Coz, James Allan, Philip L. Croteau, John Jayne, Manjula R. Canagaratna, Leah Williams, Valerie Gros, Andre S. H. Prevot, Olivier Favez & Evelyn Freney (05 Nov 2024): Evaluation of aerosol chemical speciation monitor response to different mixtures of organic and inorganic aerosols, *Aerosol Science and Technology*, DOI: [10.1080/02786826.2024.2412999](https://doi.org/10.1080/02786826.2024.2412999)

To link to this article: <https://doi.org/10.1080/02786826.2024.2412999>



© 2024 The Author(s). Published with license by Taylor & Francis Group, LLC



[View supplementary material](#)



Published online: 05 Nov 2024.



[Submit your article to this journal](#)



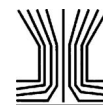
Article views: 186






[View related articles](#)



[View Crossmark data](#)



Evaluation of aerosol chemical speciation monitor response to different mixtures of organic and inorganic aerosols

Luminița Mărmureanu^{a,b} , Cristina Antonia Marin^{a,c}, Jeni Vasilescu^a, Jean-Eudes Petit^{d,e}, Tanguy Amodeo^{e,f}, Francois Truong^{d,*}, Bogdan Antonescu^{g,h}, Maria Cruz Minguillonⁱ, David C. Green^j, Bibi Zainab^k, Jurgita Ovadnevaite^l, Thomas Elste^m, Esther Cozⁿ, James Allan^k, Philip L. Croteau^o, John Jayne^o, Manjula R. Canagaratna^o, Leah Williams^o , Valerie Gros^{d,e}, Andre S. H. Prevot^p, Olivier Favez^{e,f}, and Evelyn Freney^{e,q} 

^aNational Institute of Research and Development for Optoelectronics INOE 2000, Magurele, Romania; ^bNational Institute for Research and Development in Forestry "Marin Dracea", Voluntari, Romania; ^cExtreme Light Infrastructure-Nuclear Physics, "Horia Hulubei" National Institute for Physics and Nuclear Engineering, Magurele, Romania; ^dLaboratoire des Sciences du Climat et de l'Environnement (LSCE), CNRS-CEA-UVSQ, Gif-sur-Yvette, France; ^eAerosol Chemical Monitor Calibration Center (ACMCC), Gif-sur-Yvette, France; ^fINERIS, Parc Technologique ALATA, Verneuil-en-Halatte, France; ^gFaculty of Physics, University of Bucharest, Magurele, Ilfov, Romania; ^hNational Institute for Earth Physics, Măgurele, Ilfov, Romania; ⁱInstitute of Environmental Assessment and Water Research (IDAEA-CSIC), Barcelona, Spain; ^jEnvironmental Research Group, MRC-HPA Centre for Environment and Health, King's College London, London, United Kingdom; ^kSchool of Earth and Environmental Sciences, The University of Manchester, Manchester, United Kingdom; ^lSchool of Natural Sciences, Physics, Center for Climate and Air Pollution Studies, Ryan Institute, University of Galway, Galway, Ireland; ^mDeutscher Wetterdienst, Meteorologisches Observatorium Hohenpeißenberg, Hohenpeißenberg, Germany; ⁿDepartment of the Environment, Centre for Energy, Environment and Technology Research (CIEMAT), Madrid, Spain; ^oAerodyne Research Inc. (ARI), Billerica, Massachusetts, USA; ^pPaul Scherrer Institute (PSI), Villigen, Switzerland; ^qCNRS-University Clermont Auvergne, Laboratoire de Météorologie Physique (LaMP), Aubière Cedex, France

ABSTRACT





As national air quality networks and international research infrastructures, such as ACTRIS (EU) and ASCENT (US), continue to expand, the deployment of online aerosol chemistry measurements increases worldwide. These research infrastructures are focused on the ability to compare atmospheric properties from one region to another, making it crucial to understand instrument operation in various settings. This paper is part of a series of publications dedicated to better understanding the operation of these instruments using a series of laboratory tests. A particular focus was made on evaluating the organic aerosol (OA) measurement performance of six Aerosol Chemical Speciation Monitors (ACSMs) when sampling known mixtures of organic and inorganic aerosols and in ambient air. The study focuses on assessing the impact of instrument-to-instrument variability on ACSM data processing as well as identifying and quantifying the previously identified $m/z44/\text{NO}_3$ artifacts that can affect the accuracy of the measurements. A high degree of variability was observed in instrument measurements of the $m/z44/\text{NO}_3$ artifact when compared to results obtained two years earlier (e.g., an increase from ~ 0 in 2016 to 0.16 in 2018 or a decrease from 0.12 in 2016 to 0.05 in 2018), confirming the need for frequent evaluation and quantification during calibration. This study underlines that the product between organic aerosol relative ionization efficiency and the instrument collection efficiency value is instrument dependent and that the variability in these values (1.78 ± 0.35) should be considered when estimating the measurement uncertainties. Using a range of specific compounds, an average RIEOA for levoglucosan (1.29 ± 0.23) close to the default value commonly used in ACSM was determined, obtaining a value more specific to each instrument. This study provides valuable information for the calibration and operation of ACSM instruments, ensuring that future studies can build on this work to evaluate and improve instrument performance.

ARTICLE HISTORY


Received 10 November 2023
Accepted 24 September 2024

EDITOR

Jingkun Jiang

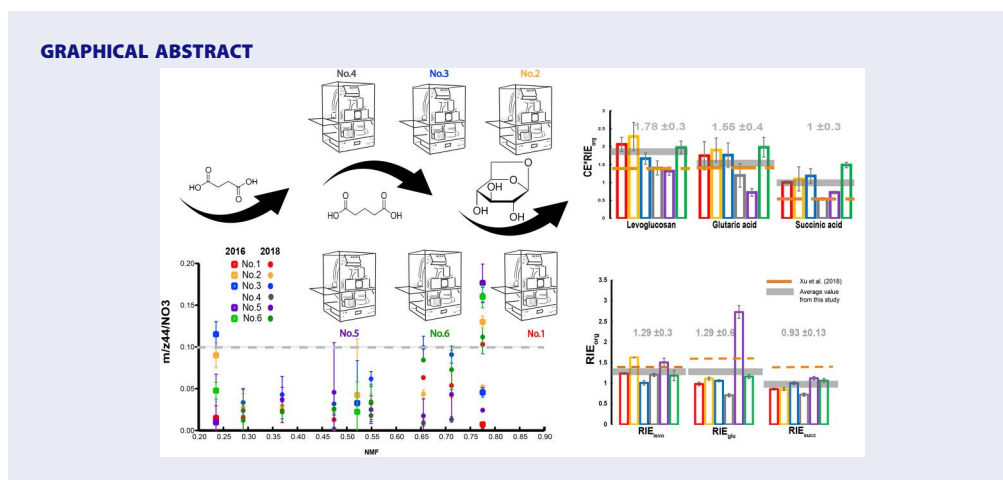
CONTACT Evelyn Freney  evelyn.freney@uca.fr  Laboratoire de Meteorologic Physique, CNRS-Universitd Blaise Pascal, Clermont Ferrand, France; Cristina Antonia Marin  cristina.marin@eli-np.ro  Extreme Light Infrastructure-Nuclear Physics, "Horia Hulubei" National Institute for Physics and Nuclear Engineering, Str. Reactorului 30, 077125 Magurele, Romania.

*Current affiliation: Laboratoire Rhéologie et Procédés, Université Grenoble Alpes, Gières, France.

 Supplemental data for this article can be accessed online at <https://doi.org/10.1080/02786826.2024.2412999>.

© 2024 The Author(s). Published with license by Taylor & Francis Group, LLC

This is an Open Access article distributed under the terms of the Creative Commons Attribution License (<http://creativecommons.org/licenses/by/4.0/>), which permits unrestricted use, distribution, and reproduction in any medium, provided the original work is properly cited. The terms on which this article has been published allow the posting of the Accepted Manuscript in a repository by the author(s) or with their consent.



1. Introduction

Atmospheric aerosols have a significant influence on the radiative budget of the Earth. Their size, as well as their chemical composition, can influence the climate directly through the scattering (cooling effect) or absorbing radiation (heating effect) of the atmosphere (IPCC 2021). Aerosol particles, also called particulate matter (PM), originate from primary aerosol sources in the boundary layer and from new particle formation in the free troposphere. In the lower troposphere, they can impact the biogeochemical cycle, atmospheric chemistry and reactivity, visibility, and human health. These particles are classified according to their size, as PM₁₀ (PM less than 10 microns in aerodynamic diameter), PM_{2.5} or PM₁. Submicron particles, which contribute 50–80% of PM_{2.5} mass, are those that have the highest impact on human health (Johannesson et al. 2007; Daellenbach et al. 2020). Organic aerosols (OA) account for a large proportion of submicron aerosol and often contribute more than 70% of the total PM₁ mass (Zhang et al. 2007; Jimenez et al. 2009; Chen et al. 2022), underlining the need for knowledge on the chemical characterization of PM, especially as OA are composed of an overwhelming number of primary and secondary compounds.

The atmospheric chemical composition of PM can either be determined using offline (e.g., Belis et al. 2013) or online methods (e.g., Canagaratna et al. 2007). The principal advantage of using the offline methods lies in their ability to provide detailed analysis of a wide range of chemical compounds. In contrast, online methods, offer a high temporal resolution, minimizing the artifacts that can result from chemical reactions involving reactive compounds or from the evaporation of volatile compounds. Advances in aerosol mass spectrometry (AMS) over

the last two decades have enabled the determination of aerosol chemical composition with high time resolution, providing information on various chemical species and their evolution in the atmosphere. One of the most widely used AMS instruments is the Aerosol Chemical Speciation Monitor (ACSM), developed for long-term autonomous sampling. These instruments are optimized for the non-refractory component of the particles (organics, chloride, ammonium, sulfate and nitrate) and can be operated as PM₁ instruments or PM_{2.5} instruments. Other commercially available instruments, like online thermo-optical methods are used to determine total organic carbon (OC), without chemical information about the types of organics, while online ion chromatography devices are commonly used to determine inorganic salts only. Aerosol mass spectrometers are currently the only instruments available that can derive information simultaneously on both inorganic and organic non-refractory compounds (Ng et al. 2011; Fröhlich et al. 2015). These instruments, specifically the ACSM, are operated at observatory sites throughout Europe (Bressi et al. 2021; Chen et al. 2022) within the ACTRIS (Aerosol, Clouds, and Trace gases Research Infrastructure) program (www.actris.eu) and in the United States of America within ASCENT (Atmospheric Science and mEasurement NeTwork, <https://research.gatech.edu/>). They are additionally deployed as part of air quality networks in several countries.

Given the growing interest in ACSM measurements, and to ensure the comparability of the data, it is necessary to ensure that these instruments provide high quality standardized measurements and follow recommended calibration procedures (Freney et al. 2019; Crenn et al. 2015; Fröhlich et al. 2015). It is also essential to understand the response of these

instruments to different atmospheric species. Within ACTRIS, the Aerosol Chemical Monitor Calibration Centre (ACMCC) (Crenn et al. 2015; <https://www.actris-ecac.eu/units.html>) is responsible for developing and implementing these harmonized procedures within the different research facilities.

Calibration protocols are designed to establish instrument sensitivity to the different species, and to convert raw ion signals into ambient mass concentrations. For the ACSM, the primary calibration to determine an ionization efficiency (IE) for nitrate species is performed with ammonium nitrate particles of known size. The sensitivity to other inorganic species is determined relative to nitrate (relative ionization efficiency, RIE) using ammonium nitrate (AN) particles or ammonium sulfate (AS) particles for RIE_{NH_4} and RIE_{SO_4} , respectively. Given the complexity of the OA composition, it is difficult to provide a calibration procedure for RIE_{OA} that is general enough to represent the range of organic molecule mixtures found in the atmosphere. Thus, a default RIE_{OA} value of 1.4 is commonly used (Xu et al. 2018; Nault et al. 2023).

Previous studies (Pieber et al. 2016; Freney et al. 2019) showed that nitrate salts, especially NH_4NO_3 , can lead to the formation of non-OA derived CO and CO_2 ion signals within the ACSM, resulting from the reaction of inorganic salts with carbonaceous material already deposited on the vaporizer. A high fraction, more than 50%, of particulate NO_3 , especially during pollution episodes, may therefore lead to an artificial increase in m/z 44 signal (CO_2^+), leading to an overestimation of oxygenated organic aerosols (OOA) and their oxidation properties. Pieber et al. (2016) proposed a methodology to correct for the interference in the m/z 44 signal using results obtained during instrument calibration with pure ammonium nitrate particles to refine OOA measurements. Subsequently, Freney et al. (2019) showed that the intensity of the m/z 44 artifact depends on the mass fraction of NO_3 in inorganic mixture (AN/AS) calibration particles. As a result, when nitrate constitutes only a small fraction of total aerosol loading in ambient air, the resulting overestimation of organic aerosols in ambient measurements is estimated to be no more than a few percent.

ACMCC focuses on comparing the responses of multiple ACSM instruments to the same input aerosol from both controlled lab and field ambient conditions. The first and second intercomparisons focused on multi-instrument variability for ambient conditions or laboratory conditions, but with only inorganic mixtures (Crenn et al. 2015; Fröhlich et al. 2015; Freney

et al. 2019). Xu et al. (2018) focused on laboratory instrument response on organic and inorganic mixtures, but only for one instrument.

This study extends previous work by measuring organic relative ionization efficiencies for pure and binary (organic-ammonium nitrate) mixtures and by examining the magnitude of the m/z 44 artifact for organic-ammonium nitrate mixtures. This was followed by a two-week intercomparison of six instruments sampling ambient air.

2. Methodology

The experiments presented in this work were organized at the ACMCC, located at the SIRTa research facility (Site Instrumental de Recherche par Télédétection Atmosphérique, (48.713°N and 2.208°E, about 20 km south of Paris city center, France; Petit et al. 2015) during November 2018 to January 2019. The work consisted in performing a series of calibrations and ambient measurements on six ACSM (Q-ACSM) instruments equipped with quadrupole mass spectrometers (Q-ACSM).

The ACSM is a robust instrument designed for long term field measurements. Best practice suggests a weekly check of instrument operation, and (at least) biannual calibration (<http://www.actris-ecac.eu/pmc-non-refractory-organics-and-inorganics.html> accessed 18 June 2024). The principle of the Q-ACSM (further referred to as the ACSM) is based on ambient aerosol collection through an aerodynamic inlet and then vaporization on a heated surface (600 °C). The resulting vapor is analyzed using electron impact ionization (70 eV) quadrupole mass spectrometry (Canagaratna et al. 2007). All ACSM instruments involved in the experiment were equipped with a standard vaporizer; five out of six instruments had inlets designed for submicronic particles ($PM_{1.1}$), and one instrument was equipped with a $PM_{2.5}$ inlet (No. 4).

This work is divided into two parts, the first focusing on laboratory experiments to better characterize instrument-to-instrument variability with controlled monodisperse particles of ammonium nitrate, ammonium sulfate and a series of organics (glutaric and succinic acids and one sugar: levoglucosan), as well as mixtures of the organics with varying mass fractions of ammonium nitrate. This data yielded information on the effective relative ionization efficiency and the m/z 44 artifact. The second part involved ambient sampling period for all instruments, with a common period of two weeks for the multi-instrument intercomparison. For ambient measurements, the

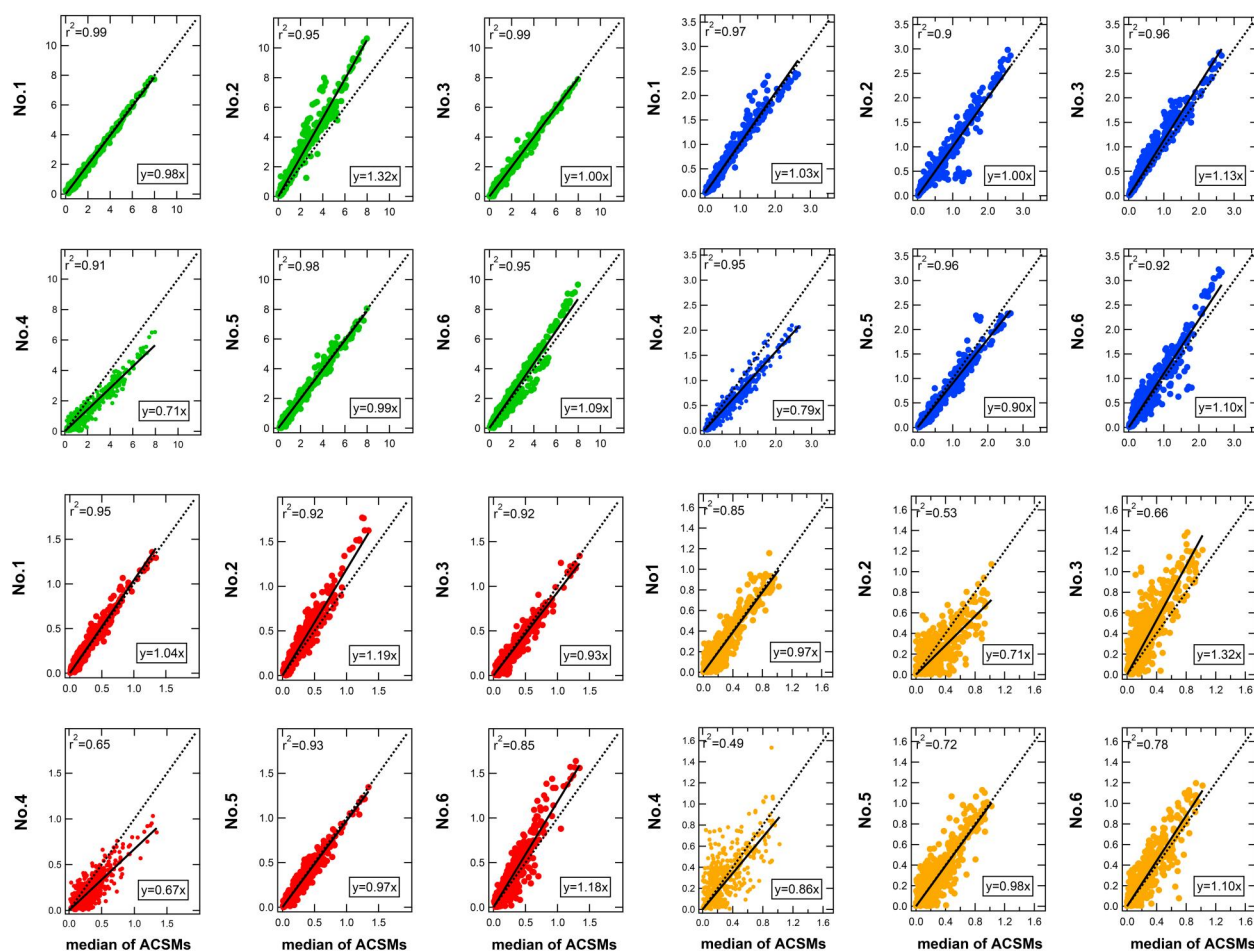


Figure 1. Intercomparison for two weeks of common period used further for SA; Org (green), NO_3 (blue), SO_4 (red), NH_4 (orange) concentration for each instrument versus the median concentration from all six instruments. These concentrations were calculated using the default RIEs for organics and the values determined during calibration for inorganics, as outlined in Table S1.

variability of derived chemical species concentrations (i.e., organics (Org), nitrate (NO_3), sulfate (SO_4), ammonium (NH_4) and chloride (Chl) were investigated. Also, the subsequent source apportionment for organics derived from each instrument data set was evaluated.

2.1. Aerosol chemical speciation monitors

As part of the requirements for instruments operating within the ACTRIS infrastructure, all instruments were calibrated at the Aerosol Chemical Monitor Calibration Center (ACMCC, <https://www.actris-ecac.eu/19-11-to-23-11-acsm-2018-1-.html>, accessed 18 June 2024).

This calibration was based on recommendations in the ACTRIS Standard Operating Procedure (SOP, <http://www.actris-ecac.eu/pmc-non-refractory-organics-and-inorganics.html>, accessed 29 August 2024), (Freney et al. 2019). The resulting calibration factors are given in Table S1. Note that the IE_{NO_3} for the Q-

ACSM is expressed as a response factor (RF) in units of $\text{amps}/(\mu\text{g}/\text{m}^3)$. The calibration report for each instrument is available on the ACTRIS ECAC site (<http://www.actris-ecac.eu/19-11-to-23-11-acsm-2018-1-.html>, accessed 18 June 2024).

The agreement of each of these instruments with the median measurement for a subsequent ambient sampling period of two weeks is shown in Figure 1 and illustrates variability between instruments of less than $\pm 30\%$, which meets the ACTRIS ACMCC “calibration standards” (Crenn et al. 2015; Freney et al. 2019).

2.2. Laboratory experiments

To quantify the ACSM response to different organic species, three different organic compounds were chosen: succinic acid ($\text{C}_4\text{H}_6\text{O}_4$, Sigma-Aldrich, purity 99%), glutaric acid ($\text{C}_5\text{H}_8\text{O}_4$, Sigma-Aldrich 99%) and levoglucosan ($\text{C}_6\text{H}_{10}\text{O}_5$, Sigma-Aldrich 99%). These organic acids glutaric and succinic acid and the sugar

levoglucosan were chosen as they are thought to represent dominant oxygenated organic aerosol and biomass burning aerosol in the atmosphere (Kawamura and Bikkina 2016). The choice of these oxygenated compounds is very relevant to the dominance of secondary organic aerosols (OA) in both urban and rural areas, which constitute an average of 71.1% of the overall OA content, ranging from 47.3% to 100% (Chen et al. 2022).

Previous studies have shown that acids and sugars can behave differently, in the presence of nitrate, in terms of collection and vaporizing efficiency (Huffman et al. 2005; Xu et al. 2018). These compounds were first introduced by atomizing a pure aqueous solution and then mixed in varying nitrate mass fractions by combining with AN (NH_4NO_3) (Table 1). In addition, two inorganic compounds (AN and ammonium sulfate- AS) were used as a pure solution and again as mixtures at different nitrate mass fractions to assess the instrument responses and m/z signal variability. Ultrapure water was used to dissolve inorganic salts and organic compounds, which were then atomized using N_2 gas (99.99% purity). Ultrapure water was nebulized for background measurements between different solutions. The time resolution of the measurements was 1 min and data was collected for approximately 30 min at three different particle number concentrations ($600, 1200, 1800 \text{ cm}^{-3}$), using a particle diluter.

Table 1. NO_3 mass fraction in solution for the organics and ammonium sulfate mixtures with ammonium nitrate.

| Succinic acid | Glutaric acid | Levoglucosan | Ammonium Sulfate |
|---------------|---------------|--------------|------------------|
| 0.67 | 0.65 | 0.7 | 0.77 |
| 0.57 | 0.55 | 0.63 | 0.71 |
| 0.47 | 0.45 | 0.51 | 0.65 |
| 0.39 | 0.37 | 0.37 | 0.53 |
| 0.25 | 0.26 | 0.26 | 0.47 |
| – | – | – | 0.37 |
| – | – | – | 0.29 |

The six instruments sampled from a common aerosol source, consisting of an atomizer (Model 3076, TSI), a silica gel dryer, a mixing tube, a Differential Mobility Analyzer (DMA, Model 3081, TSI) for 300 nm particle selection, a Condensation Particle Counter (CPC, Model 3775, TSI), and a Centrifugal Particle Mass Analyzer (CPMA, Model Mk2, Cambustion). The CPMA was used for some ammonium nitrate and ammonium sulfate measurements to remove multiple charged particles from the DMA output. The use of CPMA was limited for inorganic mixtures due to the unavailability of equipment for further measurements.

From the CPMA, the sampling line was split in two using Y-shaped connectors. Each sampling line was then connected to three instruments (Figure 2). Even though one of the instruments had a $\text{PM}_{2.5}$ inlet, the generated particles were not large enough to make a difference, so no additional setup was necessary.

2.3. Ambient measurements

Following the laboratory experiments, all six ACSMs sampled ambient air from December 1st to 8th and then again from December 19th to 24th. The ambient conditions during these intercomparison periods are detailed by Figure S1 in the online supplementary information (SI). They were notably characterized by positive temperatures ($10^\circ\text{C} \pm 2^\circ\text{C}$), high relative humidity with a few rain events, and prevailing westerly winds with an average intensity of about 4 m/s. The experimental setup used for these measurements is described in Figure S2. The SIRTAs instrument and one other ACSM sampled on a separate line, while the three other ACSMs equipped with PM_1 lens were grouped together after a common $\text{PM}_{2.5}$ cyclone. A third sampling line was equipped with a PM_4 cyclone for instrument No. 4 which had a $\text{PM}_{2.5}$ inlet (Zhang et al. 2017). Each ACSM was equipped with its own

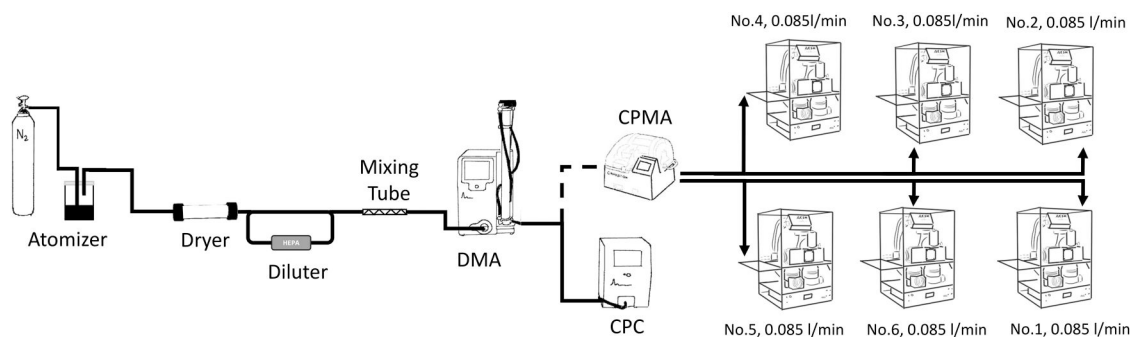


Figure 2. Schematic of the laboratory setup for binary mixtures measurements. Continuous lines represent the permanent use of equipment. The dashed line represents the occasional use of the CPMA, when needed.

Nafion dryer, and the measured humidity ranged between 20% and 40%. During the ambient sampling, one instrument (No. 2) required a filament change (between December 9th and 17th, the instrument was down). Following this filament change, a second set of standard (AN and AS) calibration was performed (Table S1). Other interruptions in the data were a result of data acquisition software malfunctions.

Each ACSM data set was analyzed separately using its specific calibration values (Table S1) using software version ACSM Local v1.6.1.1, developed in IGOR pro 6. During the measurement period, two instruments detected negative chloride concentrations. The negative chloride artifact was found to result from a negative signal difference at m/z 35 (Tobler et al. 2020). The same author reported this issue for another instrument, recommending chloride calibrations using ammonium chloride particles. These calibrations could not be performed for this experiment and so a different approach for correcting these negative values was tested (Section S.I. S5).

As a result of negative chloride concentrations (higher than the detection limit of $0.011 \mu\text{g}/\text{m}^3$, as determined by Ng et al. 2011), a constant CE of 0.5 was used, rather than calculating a composition dependent efficiency (CDCE) as described by Middlebrook et al. (2012). Furthermore, chloride measurements were not utilized. However, for instruments that did measure positive chloride, the computed ANMF (Ammonium Nitrate Mass Fraction) was consistently below 0.3. According to Middlebrook et al. (2012), a constant CE value of 0.45 should be applied in such cases, which would not affect the subsequent results. After treatment of each instrument data set, a common time frame was computed by interpolating data at the same time points with a 30 min resolution for all instruments, as described by Crenn et al. (2015).

Positive matrix factorization (PMF) (Viana et al. 2008; Karagulian and Belis 2012) was used to identify submicronic organic aerosol sources (Crippa et al. 2013; Canagaratna et al. 2015). One of the most recent and widely used approaches for PMF is the Source Finder Tool (SoFi) (Canonaco et al. 2013), based on the multi-linear engine (ME-2, Paatero 1999). SoFi is used for source apportionment (SA) to identify primary organic aerosol (POA): hydrocarbon-like organic aerosol (HOA), cooking organic aerosols (COA), biomass burning organic aerosols (BBOA), or secondary organic aerosols (SOA): more oxidized oxygenated organic aerosols (MO-OOA), less oxidized (LO-OOA) (e.g., Canonaco et al. 2013; Crippa et al. 2013;

Canonaco et al. 2021; Märmureanu et al. 2020). In this work, for each ACSM, the organic mass spectra were analyzed to identify the best factor solutions using SoFi Pro version 6G, developed in IGOR Pro software (<https://datalystica.com/sofi-pro/>, accessed February 2022). A common period of approximately two weeks is used for comparison of the PMF results. The spectra with m/z signals from 13 to 120 were down-weighted based on the signal-to-noise ratio using the step function. Typically the Q-ACSM profile spectra are truncated at m/z 100 due to uncertainty related to large correction for ion transmission, we still decide to use spectra with m/z signals up to 120 to gain as much information as possible. The analysis of the PMF solutions follows the protocol proposed by Canonaco et al. (2013, 2021) and Chen et al. (2022), based on the identification of source-dependent markers. Three factor solutions have been chosen, using bootstrap and up to 100 runs per factor. To separate the primary factors, organic spectra deconvoluted in previous studies, obtained for Paris, were used to constrain the model based on a -values with a 0.05 step from 0 to 0.3 for HOA and 0.5 for BBOA (Crippa et al. 2013; Fröhlich et al. 2015). The following criteria were used to choose the best solutions: explained variation of m/z 60 in the BBOA factor and variation of m/z 44 and m/z 60 in the OOA factor.

3. Results and discussions

3.1. Laboratory measurements

3.1.1. Assessing response to organics with different calibrants

The mass concentrations reported by Aerodyne aerosol mass spectrometer (AMS) and ACSM instruments depends on the relative ionization for that specific compound (Xu et al. 2018). However, without a separate measurement of either RIE or CE, the response of the instrument gives a measure of $\text{RIE} \cdot \text{CE}$. As discussed by Xu et al. (2018), the $\text{RIE} \cdot \text{CE}$ can be calculated by comparing the measured instrument signal response with the calculated input mass concentration. As the CPMA was not used for these experiments, the input mass concentrations were derived using assumptions related to particle density and shape (i.e., density for Levoglucosan (1.69), glutaric acid (1.43), succinic acid (1.56), and for shape (1)) (<https://www.chemspider.com/Chemical-Structure.9587432.html> - accessed 18 June 2024). Figure 3 shows a comparison between the product of CE and RIE values from Xu et al. (2018), and the $\text{CE} \cdot \text{RIE}$ measured with 6 instruments from the present work, all having standard vaporizers. $\text{RIE}_{\text{OA}} \cdot \text{CE}$

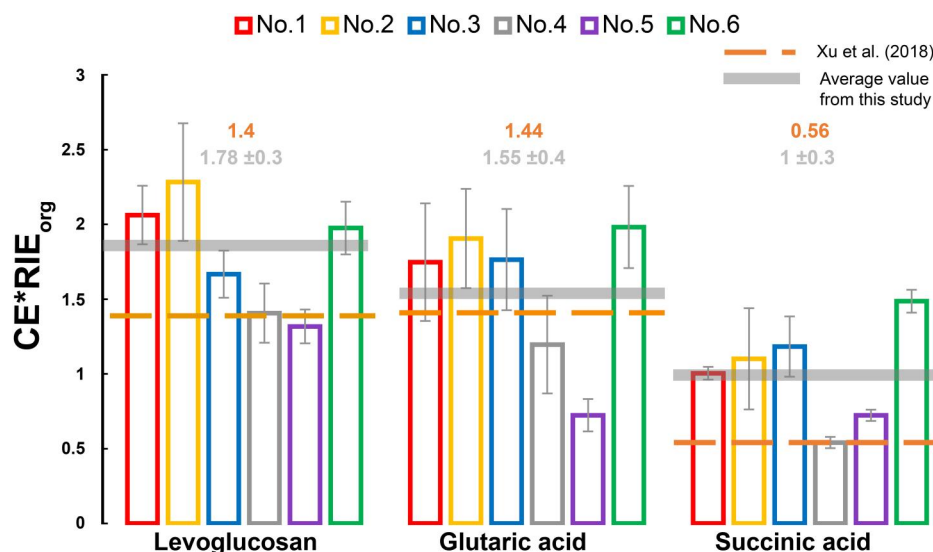


Figure 3. CE*RIE determined for pure org: levoglucosan (average 1.78 ± 0.3), glutaric acid (average 1.55 ± 0.4), and succinic acid (average 1 ± 0.3) marked with horizontal grey line. The horizontal dash lines represent the CE*RIE_{OA} results from Xu et al. (2018).

values were averaged over a range of particle concentrations (i.e., 600, 1200, 1800 cm^{-3}). The results of RIE*CE for levoglucosan, varies between 1.3 and 2.2 (with an average value of 1.78 ± 0.35) (Figure 3), and are in reasonable agreement with previous values reported in the literature for a standard vaporizer, assuming CE to be 1 for pure levoglucosan as described in Xu et al. 2018 (RIE = 1.4) and in Jimenez et al. 2016 (RIE = 1.8 ± 0.2).

In the case of glutaric acid RIE*CE, the measured values of instruments 1,2,3, and 6 agree well with each other, with Nos. 4 and 5 being much lower than the average (Figure 3). Despite these differences, the average values (1.55 ± 0.44) obtained across the 5 instruments are in good agreement with previously reported values (1.44, Xu et al. 2018; 0.9, Jimenez et al. 2016). In the case of succinic acid, all instruments have values between 0.54 (for instrument 4) and 1.48 (instrument 6), and only two instruments (4,5) are in the range of previous literature values (0.56 ± 0.13 , Xu et al. 2018; 0.4 ± 0.08 , Jimenez et al. 2016).

Performing these tests on multiple instruments under the same conditions allows us to determine instrument-to-instrument variability of RIE*CE. It is possible that the differences in CE between instruments contribute somewhat to this variability.

Xu et al. (2018) introduced the use of simple binary aerosol mixtures as a means of deriving organic RIE values independent of CE. In this method, calibrations are performed with mixtures of known ammonium nitrate/organic ratios. The nitrate is used as an

internal standard for determining the RIE of the organic species (RIE_{OA}).

The RIE_{OA} from binary mixtures is calculated based on the following equation (Equation (1)).

$$RIE_{OA} = \text{slope} (org/NO_3) \text{ vs } (MFor_{org}/MFor_{NO_3}) \quad (1)$$

where Org, NO₃ are the concentrations recorded by ACSM, and MFor_{org} and MFor_{NO₃} are their corresponding mass fractions.

The key advantage of this method is that it enables measurements of RIE without the need for simultaneous measurements of CE. While this method has been demonstrated by Xu et al. (2018) on a capture vaporizer, it has not been evaluated across multiple instruments or on standard vaporizers. The RIE_{OA} for each instrument using the ratio between organics and nitrate is presented in Figure 4.

The average value obtained across all instruments for RIE Levo is 1.29 ± 0.23 . This value is within the range (albeit 8% lower) of the default RIE_{org} value of 1.4 that is typically used in ACSM data processing. Xu et al. (2018) have shown that RIE_{OA} varies with organic oxidation state and that laboratory RIE_{OA} measured for oxidized organics is slightly higher than the default RIE_{OA} of 1.4 used for AMS/ACSM data processing. It was hypothesized to be a result of displacement reactions that can take place between the organic acids and ammonium nitrate to produce organic salts and gaseous HNO₃. However, this was not observed for the sugar/NO₃ mixtures. In this work, calculating the RIE independent of CE for this study impacted the results of both the sugars and the

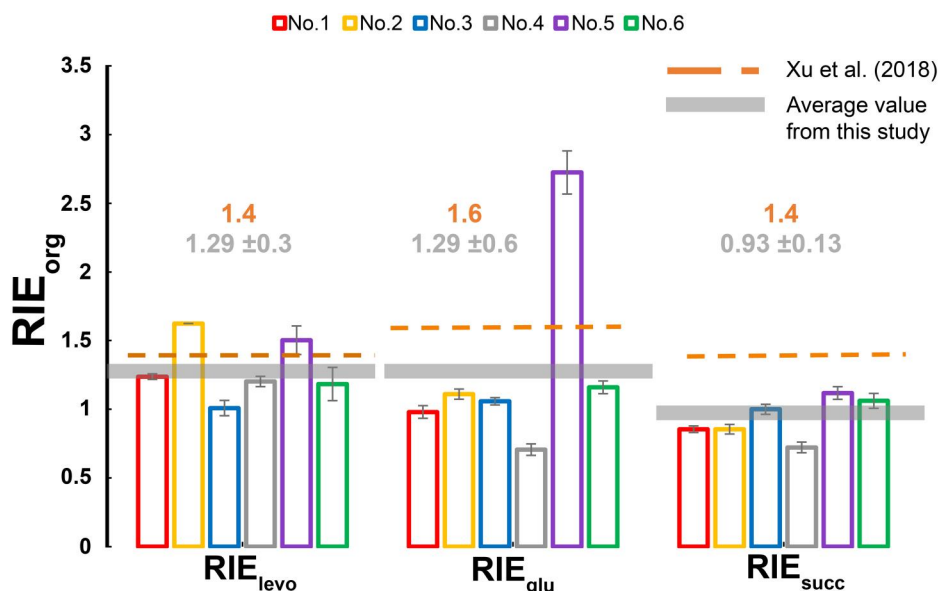


Figure 4. RIE_{OA} derived from organic/ nitrate ratios for all organic compounds: levoglucosan (average 1.29 ± 0.2), glutaric acid (average 1.29 ± 0.6), and succinic acid (average 0.93 ± 0.13) marked with horizontal grey line. The dashed lines represent RIE values calculated from the Xu et al. study.

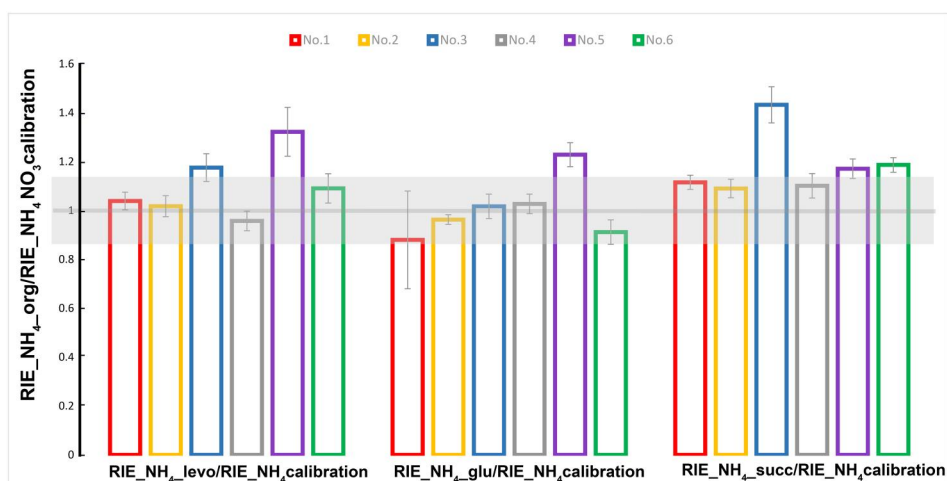


Figure 5. Ratio of RIE_{NH4} determined from a binary mixture of levoglucosan, succinic, glutaric, and pure ammonium nitrate to RIE_{NH4} determined from AN calibration. Grey horizontal shadows represent the 17% limit and the errors bars represent the propagated RIE_{NH4} determined from organic/inorganic solutions.

acid mixtures (Figure 4). This approach provided more consistent RIE values of RIE for all organic mixtures, compared to the pure solution method, which showed much lower values for succinic acid (Figure 3). The RIE values for the sugar (i.e., RIE_{levo}) are much closer to the Xu et al. (2018) average value than the RIE values observed for the acids (i.e., RIE_{glu} and RIE_{succ}).

The displacement reactions in the binary solutions can also be investigated by examining RIE_{NH4} for the binary solutions and comparing with values obtained from NH₄NO₃ calibration.

The RIE_{NH4} are calculated based on the approach described by Tobler et al. (2020) (Equation (2)).

$$RIE_{NH_4} = \frac{\text{slope}(\text{Signal}_{NH_4} \cdot RIE_{NO_3} \cdot MW_{NO_3})}{(\text{Signal}_{NO_3} \cdot MW_{NH_4})} \quad (2)$$

where MW_{NO₃} and MW_{NH₄} are the molecular weights for NO₃ and NH₄, respectively.

The ratios of RIE_{NH4} values obtained using organic/inorganic mixtures are illustrated in Figure 5,

relative to the RIE_{NH_4} values calibrated with pure ammonium nitrate.

The average RIE_{NH_4} ratios determined across these different binary mixtures are similar. The mean ratio obtained for all organic compounds is 0.97 ± 0.06 , ranging from 0.89 ± 0.30 for glutaric acid to 1.05 ± 0.36 for succinic acid. Xu et al. (2018) reported higher but more stable RIE values from the acid/ NO_3 mixtures compared with those calculated from pure NH_4NO_3 solutions. In this work, the RIE_{NH_4} calculated from mixtures has a variability of a similar range of variability as that calculated across all instruments during previous calibrations ($\pm 17\%$) (<https://www.actris-ecac.eu/reports.html>). In the organic/inorganic mixture experiments using levoglucosan, five out of six instruments fall within this 17% range, while instrument No. 5, has a higher variability of 30% from the mean of all the instruments. Similarly, for the glutaric acid binary mixture, it was observed that also for five instruments (Nos. 1, 2, 3, 4, 6), RIE_{NH_4} ratio is stable and falls within the $\pm 17\%$ variability. For instrument No. 5 we obtained a slightly higher value (22%) than the RIE calculated using pure AN. For the succinic acid/inorganic mixture, only one instrument (No. 3) had a RIE_{NH_4} higher than in the expected range of 17% determined from pure AN from successive calibrations.

Having a large number of instruments offers the opportunity to investigate different approaches for calculating organic RIE, and demonstrates the variations that can occur across different instruments. The validity of these methods is confirmed through cross verification with the RIE of NH_4 in pure solutions. Despite the potential concern of acid displacement reactions, no clear differences were noted in this study. As suggested by Xu et al. (2018), these experiments and tests can be easily implemented as part of calibration exercises.

3.1.2. Assessment of m/z 44 artifact in the presence of ammonium nitrate and ammonium sulfate mixture

Previous studies highlighted the variability in response to organic species in different ACSMs under the same atmospheric conditions, which is thought to be essentially a result of the variability at the signal m/z 44 (Figure S3) (Crenn et al. 2015). Despite this variability, the resulting organic factors resolved from source apportionment analyses were not impacted (Fröhlich et al. 2015). Pieber et al. (2016) demonstrated that some instruments can generate a non-organic aerosol m/z 44 signal, induced by processes like thermal decomposition or particle reactions on the vaporizer,

while sampling inorganic salts (notably ammonium nitrate). Thus, Pieber et al. (2016) recommended regularly evaluating the relationship between the m/z 44 signal and relevant salts using pure ammonium nitrate salt aerosol.

The Pieber artifact was evaluated by Freney et al. (2019) during the 2016 inter-comparison exercise for inorganic mixtures with varying nitrate mass fractions. Their findings demonstrated that this artifact is chemistry-dependent and becomes significant in the m/z44 signal and subsequent in the f44 and O:C interpretation, only at high nitrate fractions. During this work, five out of six instruments that participated in the 2016 and 2018 intercomparisons were available, enabling the evaluation of this artifact over time. In Figure 6, the results obtained in the 2016 and 2018 inter-comparisons are plotted together. In the 2016 intercomparison, the measurements were conducted on three different NO_3 mass fractions (NMF) (0.235, 0.521, 0.775), while in 2018, six NMF (Table 1) were used for the inorganic mixtures.

Similar to Freney et al. (2019), the results from 2018 show an increase of the artifact above an NMF of 0.5, a concentration that is not common for ambient conditions (Zhang et al. 2007; Bressi et al. 2021).

At the highest NMF, i.e., with pure AN, three out of the six instruments exhibit a significant (defined as $m/z\ 44/NO_3 > 0.10$) Pieber artifact. This artifact differs from the previous observations on the same instruments in the 2016 intercomparison (Figure 6). In 2016, the artifact was present in instruments 2 (0.12), 5 (0.17) and 6 (0.16), while in 2018, it was found in 1 (0.10), 3 (0.16), and 6 (0.11). Pieber et al. (2016) suggested that the vaporization process and interactions between oxidants resulting from NH_4NO_3 decomposition and vaporizer residues lead to CO_2 production. This highlighted how the history of the vaporizer and exposure to different aerosols might influence further behavior. For example, one of the instruments (No. 2.) that had an artifact value of 0.12 in 2016 (Freney et al. 2019) had a relatively low value of 0.05 in 2018. During the two years between inter-calibration campaigns, there were no events with major maintenance (e.g., change of filament or vaporizer) procedures that could induce changes in this artifact. A possible explanation could be related to a gradual cleaning over time from previous exposures before 2016.

Further investigation into the evolution of this artifact is recommended, as no evidence is available to explain why the artifact decreases over time. The dependence of this artifact on exposure to different aerosol compositions is not yet sufficiently understood,

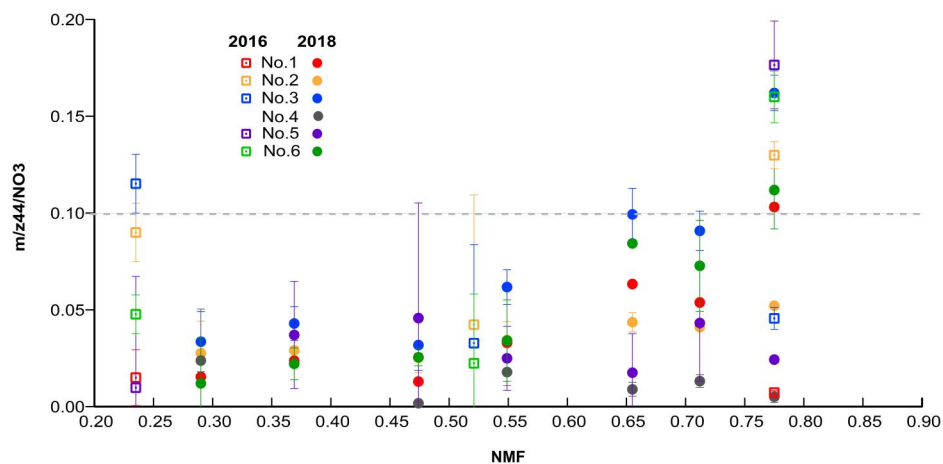


Figure 6. $m/z44/NO_3$ artifact as a function of NMF for ACSM instruments during AN-AS inorganic mixtures experiments, data obtained in 2016 (open squares Freney et al. 2019) and 2018 (solid circles, present study). A ratio above 0.1 (dotted line) is considered a significant Pieber effect.

and these measurements underscore the need for verification of the Pieber artifact for each given instrument.

3.1.3. Assessment of m/z 44 artifact in internally mixed organic-inorganic (ammonium nitrate) aerosol particles

In the following sections, an assessment of how this artifact varies with different mixtures of organic/inorganic aerosols will be discussed. The impact of this artifact on m/z 44 is evaluated through analysis of m/z 44 to NO_3 ratios as well as $f44$ variability as a function of NMF.

In inorganic/organic mixtures, the presence of the $m/z44$ artifact associated with the NO_3 mass fraction can be identified if the $m/z44$ signal from pure organic compounds can be isolated and removed (Figure S4). The following steps were taken separately for each acid or sugar and each instrument:

- (a) To determine the $m/z44$ contribution from each of the pure organic solutions, the average $m/z44$ (from pure solution measurements) was calculated for each instrument;

$$m/z44' = \text{Avg}(m/z44_{\text{pure}})$$

- (b) In the pure organic solutions and in the organic mixture solutions, the m/z 44 signal was removed, and a new time series for organic mass concentration was created and named Org_no44_pure and Org_no44 , respectively:

$$[Org_no44] = [org] - m/z44$$

$$[Org_no44_pure] = [org_pure] - m/z44'$$

- (c) The next step was to estimate an $f44$ that is representative of a pure organic solution. This $f44'$ was

determined by dividing $m/z44'$ (from a) by the Org_no44_pure selecting just pure measurements time stamp for each instrument (from b).

$$f44' = m/z44' / Org_no44_pure$$

- (d) This value, $f44'$ for pure organic (from c), was then multiplied by the total organic time series without m/z 44 (Org_no44) for each of the mixtures.

$$m/z44 \text{ for extraction} = f44' * Org_no44$$

- (e) From this, we obtained the expected m/z 44 for the pure organic solutions, and from here, it was possible to estimate a possible $m/z44$ artifact through comparison with the m/z measured in the mixture $m/z44_{\text{mix}}$.

$$m/z44_artifact = m/z44_{\text{mix}} - m/z44 \text{ for extraction}$$

- (f) Then to calculate the $m/z44/NO_3$ ratio for comparison with previous studies, the m/z 44_artifact (from e) was divided by the measured NO_3 signal.

The variability in this calculated artifact determined during binary mixtures and pure AN is shown in Table 2. The artifact for pure AN (Table 2, column (2)) shows that instrument No. 3 presents the highest artifact value (0.16), followed by instrument No. 6 (0.11), and then instrument No. 1 (0.10). For instruments Nos. 3 and 6, they also had the highest artifacts at lower NMF (<0.55) for glutaric and succinic acid. Despite these organic mixture artifacts were low (≤ 0.10), they were still several times higher than those measured for inorganic solutions at lower NMF. Comparing the values from pure ammonium nitrate (in column 2) and organic solutions (columns (4)-levoglucosan, (5)-glutaric acid, (6)-succinic acid), we can see that this artifact is not consistent for all mixtures.

Table 2. The behavior of $m/z_{44}/NO_3$ in different organic and inorganic mixtures and for pure an.

| Instrument number (No.) (1) | AN Pure (2) | AN-AS NMF < 0.5 (3) | AN-levoglucosan NMF 0.371–0.514 (4) | AN-glutaric acid NMF 0.369–0.549 (5) | AN-succinic acid NMF 0.391–0.566 (6) |
|--------------------------------|-------------------|---------------------------|--|---|---|
| 1 | 0.10 | 0.017 | 0.08 | 0.06 | 0.05 |
| 2 | 0.05 | 0.027 | 0.09 | 0.04 | 0.03 |
| 3 | 0.16 | 0.036 | 0.11 | 0.07 | 0.05 |
| 4 | 0.005 | 0.007 | 0.04 | 0 | 0.01 |
| 5 | 0.02 | 0.016 | 0.09 | 0.07 | 0.04 |
| 6 | 0.11 | 0.019 | 0.14 | 0.1 | 0.03 |

The values for the organic artifact represent the average of m/z_{44} to NO_3 ratio between specific NMF. Bolded numbers represent the values above 0.1 threshold used by Pieber et al. (2016).

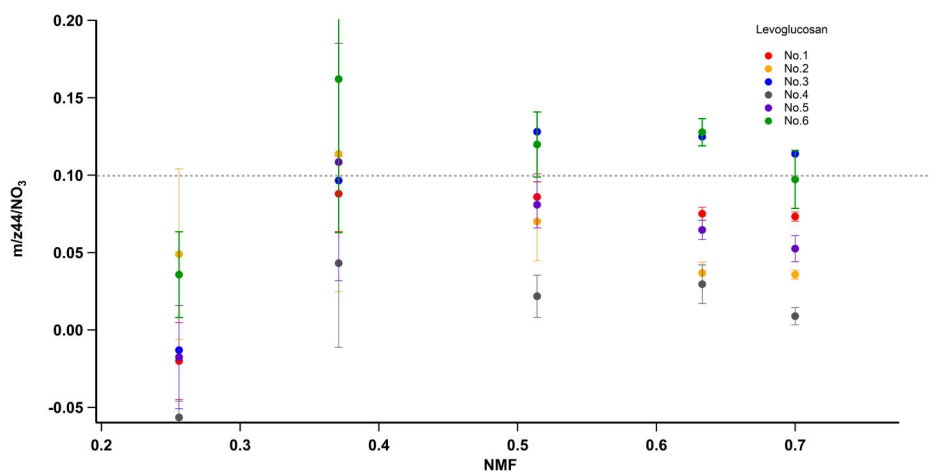


Figure 7. $m/z_{44_artifact}/NO_3$ as a function of NMF. The dotted line represents the Pieber threshold of 0.1.

For example, instrument No. 6 shows the highest artifact for levoglucosan (0.14) and glutaric acid (0.1), but not for succinic acid (0.03).

While the behavior of the acid mixtures resembled that of sugar mixtures, the presence of potential acid displacement reactions in the acid/ NO_3 binary solutions could likely complicate further interpretation. Consequently, the m/z_{44} artifact for the acid mixtures is not investigated further.

Figure 7 shows the $m/z_{44_artifact}/NO_3$ for the levoglucosan mixture plotted as a function of NMF to better evaluate how the artifact behaves in different instruments.

Two of the instruments (Nos. 3, 6) with Pieber artifact during the pure AN (Table 2, column 2) experiments, show the highest $m/z_{44_artifact}/NO_3$ signal for the mixed solutions. However, according to the $m/z_{44_artifact}/NO_3$ ratio instruments 3 and 6 are clearly influenced by this artifact at low NMF (between 0.3 and 0.5), and this artifact persists even at high NMF. These observations indicate that these instruments showing an artifact in pure NMF solutions also display it in organic mixtures. Importantly, the artifact appears at lower and more atmospheric relevant mass fractions.

This method of calibrating with internally mixed binary solutions with sugars could provide a means of identifying instruments with significant Pieber effects

that need to be corrected for further analyses like SA. We recommend testing instruments for an initial m/z_{44} artifact (using a standard ammonium nitrate calibration) followed by more specific tests so to integrate a correction into the fragmentation table. In the following paragraphs, we explore the different methods of correcting for these artifacts based on both laboratory and ambient measurements.

The factors identified (Table 2, column 4) in the current study show small differences compared to those identified by the methodologies described in Pieber et al. (2016) (Table 2, column 2). Since the difference is small and the purpose of this paper is not to propose a new correction methodology, previously proposed correction methodologies will be used (Pieber et al. 2016; Freney et al. 2019).

To assess and standardize the response of the instruments to these binary mixtures, the corrections proposed in the literature were applied separately and compared using Equation (3)

$$\begin{aligned}
 fragorganic[44] = & 44, -fragair[44], -b \bullet 1.05 \\
 & \bullet fragnitrate[30], -b \bullet 1.05 \\
 & \bullet fragnitrate [46]
 \end{aligned} \quad (3)$$

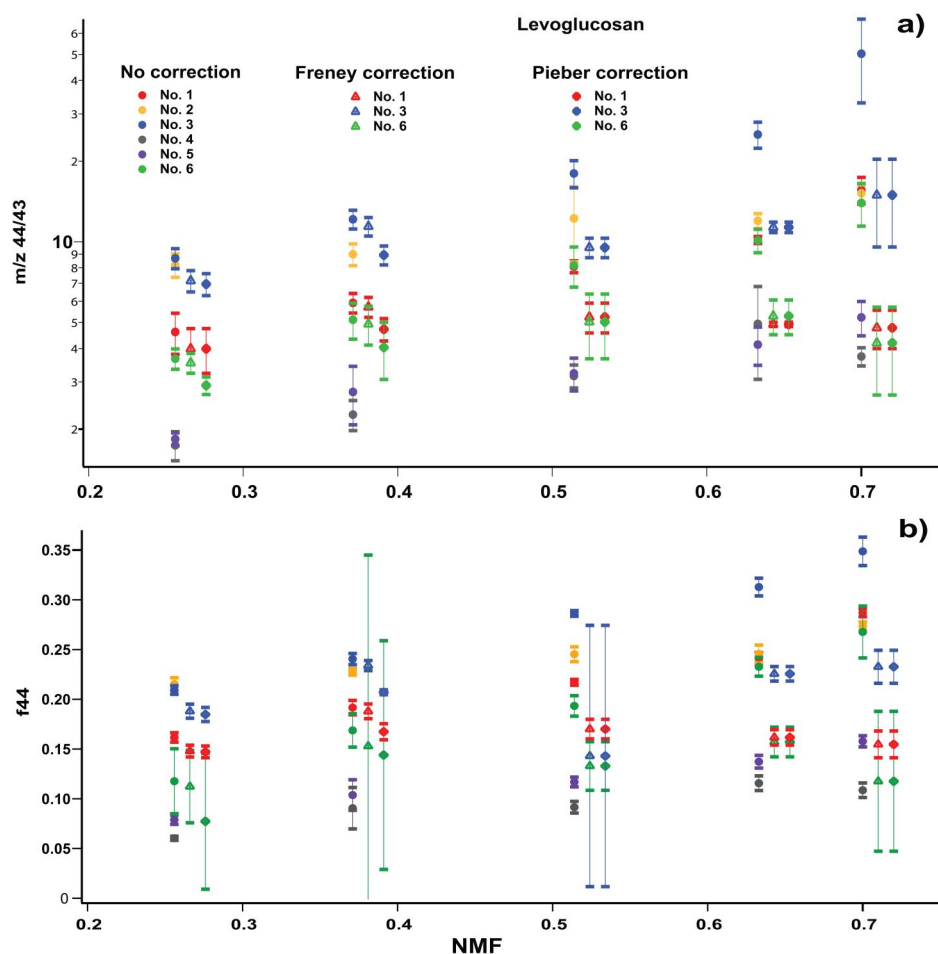


Figure 8. $m/z44/m/z43$ ratio as a function of NMF as a response of different binary mixture as follows: (a) levoglucosan-AN, without and with Pieber and Freney correction applied; and (b) $f44$ without and with Pieber and Freney correction applied.

- For Pieber correction b represent $m/z44/NO_3$ measured during pure AN calibration
- For Freney correction, the artifact is compensated depending on NO_3 MF. For NO_3 MF < 0.5 , b represents the average of the $m/z44/NO_3$ ratio calculated at these low MF. For NO_3 MF > 0.5 , a linear fit between the artifact values at MF > 0.5 , and that of pure AN is calculated.

The corrections were applied just for instruments 1, 3, and 6, for laboratory data, as these instruments showed an artifact above 0.1, during pure AN calibration (Table 2).

The instruments that are identified with the Pieber artifact have shown in all mixtures constantly higher $m/z44/43$, than the rest of the instruments (Figure 8a).

The applied correction results in a more uniform distribution of $f44$ to NMF (Figure 8b) for both applied methodologies.

The $f44$ variation across instruments Nos. 1, 3, and 6 before applying any correction ranged from 0.30 ± 0.04 (NMF 0.7) to 0.16 ± 0.04 (NMF 0.256).

After applying corrections, the values ranged from 0.17 ± 0.05 (NMF 0.7) to 0.15 ± 0.03 (NMF 0.256) with the Freney correction and from 0.17 ± 0.05 (NMF 0.7) to 0.14 ± 0.05 (NMF 0.256) with the Pieber correction. When compared to the values derived from instruments not requiring corrections, which ranged from 0.17 ± 0.08 (NMF 0.7) to 0.12 ± 0.08 (NMF 0.256), we observed comparable results across all instruments.

Given the low level of these artifacts, we propose applying the Pieber correction, using a constant artifact value. This approach is specific to these data sets where the ANMF remained less than 0.5 and the artifacts were < 0.15 . In cases of higher artifact values, or if the ANMF exceeds 0.5, it would be necessary to reevaluate this procedure. However, considering that in organic mixtures the $m/z44$. For the $f44$ from Nos. 2, 4 and 5, we did not apply any correction since the artifact value (Table 2, columns 2 and 4) is lower than the threshold value (0.1) identified by Freney et al. (2019).

The $m/z44$ artifact should be constantly assessed since this is reflected in the $m/z44/43$ ratio and subsequently in $f44/f43$ interpretations. Triangle plots of

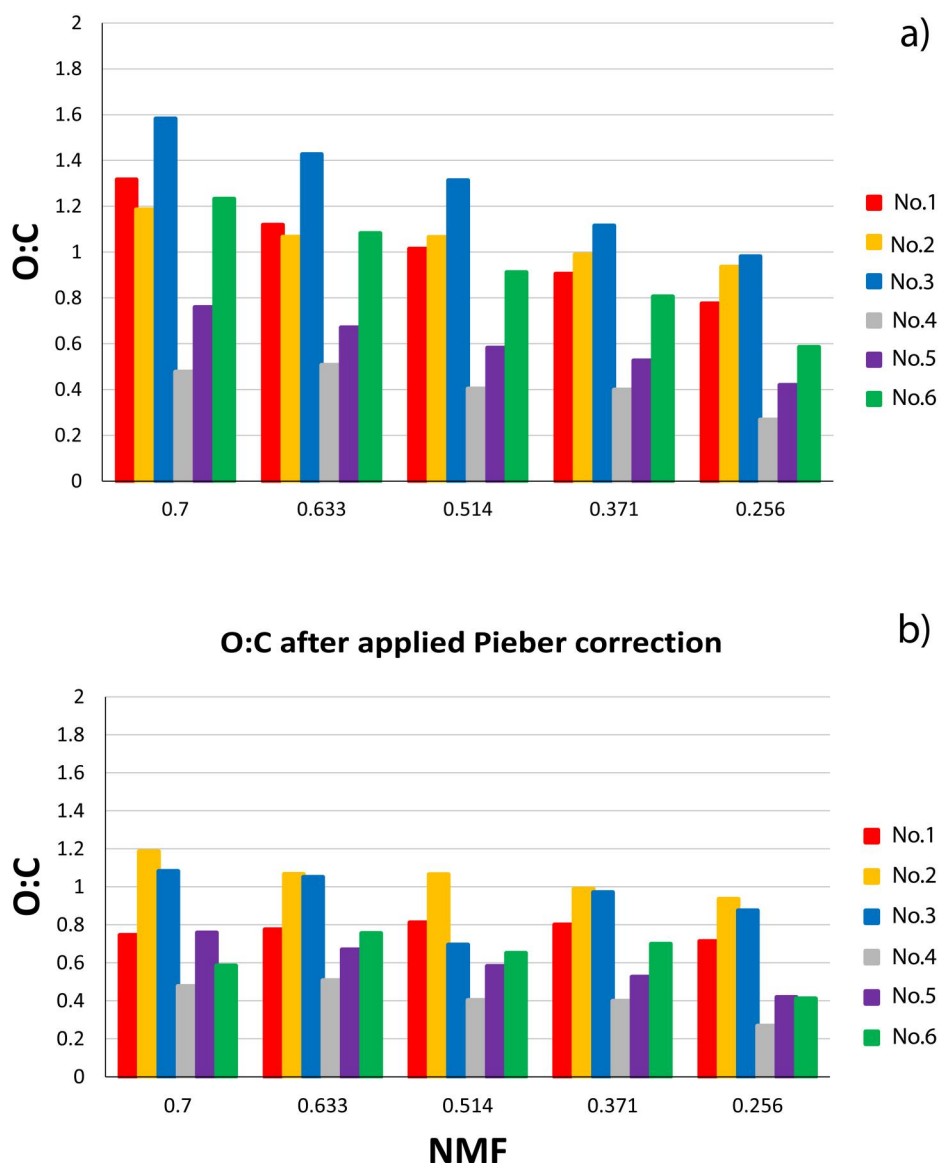


Figure 9. O:C values as a function of NMF as follows: (a) O:C determined without any correction, and (b) O:C determined after Pieber correction applied.

f44 vs. f43 are usually used to evaluate the oxidized organic compound contribution to the total organic mass (Ng et al. 2011). Although the previous ACSM inter-comparisons show good agreement between instruments in mass concentrations (Crenn et al. 2015), the f44 variability is still significant. Likewise, corresponding estimations of O:C values should be carefully interpreted. If an instrument is suspected of having a Pieber artifact, it is important to exercise caution when presenting the O:C ratios. In this work, we estimated the O:C ratios (using the method presented in Poulain et al. 2020; Equation (4))

$$O : C = 0.079 + 4.31 * f44 \quad (4)$$

As shown in Figure 9a, there is considerable variability in the O:C ratio depending on the instrument.

This variability increases with the NMF. The estimated O:C values range from 0.5 up to 1.5, values typically used to separate low oxidized OA species (BBOA) from highly oxidized species (Canagaratna et al. 2015). Applying a standard Pieber correction decreased the variability within each NMF, especially at the highest NMF (Figure 9b).

The O:C variation across instruments Nos. 1, 3, and 6 before applying the Pieber correction ranged from 1.37 ± 0.18 for an NMF of 0.7 to 0.78 ± 0.19 for an NMF of 0.256. After applying the Pieber correction, the average O:C values were 0.80 ± 0.19 for an NMF of 0.7 to 0.66 ± 0.23 for an NMF of 0.256. These values are very similar to the averages from instruments that did not require correction, which were 0.80 ± 0.3 (NMF 0.7) and 0.54 ± 0.34 (NMF 0.256).

We recommend here that for artifact values less than 0.15, a simple standard Pieber correction can be implemented into fragmentation tables. However, given the conclusions made by Freney et al. (2019), applying a correction to instruments that exhibit a high artifact ($m/z44/\text{NO}_3 > 0.15$), across all concentrations ($\text{NMF} > 0.4$), may result in an underestimation of O:C ratios.

In this context, it is recommended to view the presence of the initial m/z 44 artifact as a warning of potential influence on the aerosol organic oxidized fraction, necessitating a more detailed artifact check in organic mixtures.

3.2. Ambient measurements

3.2.1. Ambient concentrations measurements intercomparisons

Following the calibrations and laboratory studies with the mixed organic solutions, all 6 instruments were installed at the SIRTA station for an extended period of ambient air measurements (4–5 wk). The objective of this exercise was to evaluate how the response of these different instruments, observed during laboratory measurements, influenced the sampled ambient mass concentrations.

The sampling location is considered a peri-urban location and is not characterized by high local emissions (Zhang et al. 2019). The average mass concentration of NR-PM1 for the intercomparison period is $2.73 \pm 0.45 \mu\text{g}/\text{m}^3$. Org is the most abundant, at 53% followed by NO_3 with 21%. SO_4 and NH_4 have the lowest contribution, 15% and 11%, respectively. More detailed information about the instrument specific mass contribution of the measured species is illustrated in Figures 10 and S5.

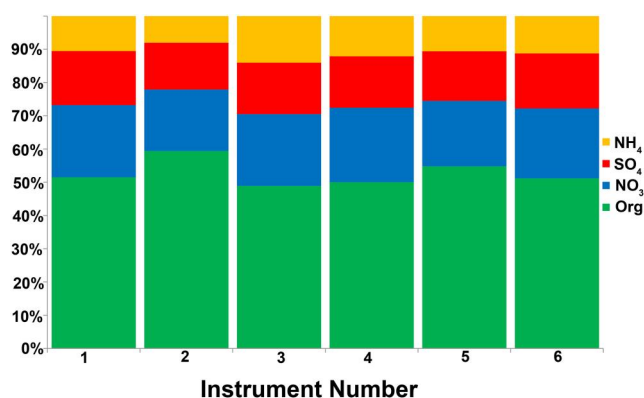


Figure 10. Average aerosol contribution per each instrument and for the common periods used in SA (supplementary material).

Unfortunately, with atmospheric mass fractions of nitrate less than 30%, we do not have optimal conditions to test the impact of the artifact on ambient concentrations. In this graph, Chl was excluded from the analysis because of negative values in two of the instruments. The negative values were not comparable between the two instruments, and the concentration did not follow the same trend. However, after a filament change (from iridium to tungsten filament type), one of these two instruments experienced positive Chl, a procedure performed during the ambient measurements. Tobler et al. (2020) described how the negative chloride is an artifact of the instrument, and can be further investigated and corrected through ammonium chloride calibrations. However, ammonium chloride calibrations were not performed for these instruments, either before or during the intercomparison. Instead, as described in S5 (RIE_{chl} adjustment), the fragmentation table for chloride was adjusted using the procedure proposed by Tobler et al. (2020). The RIE_{Chl} for instrument 2 (or 3) was adjusted from 1.3 (used as default in ACSM data processing) until the Chl mass loading agreed best with the average of instruments 1, 5, and 6.

The intercomparison between instruments is illustrated in Figure 1 for Org (without any correction applied), NO_3 , NH_4 , and SO_4 . For Org and NO_3 , good correlations are observed ($R^2 > 0.9$), while the R^2 varied from 0.65 to 0.95 for SO_4 and from 0.49 to 0.85 for NH_4 . The lower correlation coefficients measured for SO_4 and NH_4 are a result of the instrument detection threshold as previously observed by Crenn et al. (2015) and Budisulistiorini et al. (2014). In the case of SO_4 , the average concentration was $0.3 \pm 0.05 \mu\text{g}/\text{m}^3$. Additionally, we noticed that instrument No. 4 had the lowest SO_4 concentration ($0.2 \mu\text{g}/\text{m}^3$), which also happened to have the lowest value of R^2 . For NH_4 , the average concentration recorded by all devices was $0.22 \pm 0.06 \mu\text{g}/\text{m}^3$, and we observed a similar pattern between the correlation coefficient and recorded concentration.

The relative deviation to the median (RDM) derived from the slope in each plot is shown in Figure 1. The RDM for Org is around 30% (the slopes for Org ranged from 0.71 to 1.32), comparable with those found by Freney et al. (2019) (slopes between 0.63 and 1.24) and within the uncertainty associated with the instrument. The best RDM is obtained for NO_3 , (the slopes ranged from 0.79 to 1.13), which is comparable with RDM obtained by Freney et al. (2019) (slopes between 0.82 and 1.22).

The highest RDM obtained was for SO_4 (33%) in case of No. 4 and for NH_4 , No. 3 (32%) that is linked with low concentrations recorded in this period for these chemical species and also to instruments detection limits. Similarly low RDMs were reported for these species by Freney et al. (2019) and Crenn et al. (2015) (around 45% for SO_4).

Instrument No. 4, which is equipped with a $\text{PM}_{2.5}$ lens, underestimated Org, NO_3 and SO_4 concentrations. The slopes obtained are 0.71, 0.79, and 0.67, respectively. We hypothesize that this phenomenon can be attributed to the fact that $\text{PM}_{2.5}$ particles exit the lens at a significantly higher velocity compared to PM_1 . This higher velocity may result in increased particle bounce, particularly for larger particles.

For the subsequent source apportionment analysis (SA), little impact of the artifact correction was observed. This is principally a result of the low artifact values measured in this study (<0.15), but also as the atmospheric ANMF remained low (<0.3) throughout the study. For this reason, the SA analyses and the subsequent impact of the artifact correction are showed in the SI (Figures S7, S8, source apportionment).

4. Conclusions

The primary goal of this work is to provide insights into the response of ACSM instruments and to more accurately evaluate previously identified artifacts. In the long-term, this information can enhance data interpretation, and ensure the interoperability of these measurements within atmospheric observational networks and infrastructures. The efforts to understand the processes that occur during the operation of aerosol mass spectrometers and the behavior of certain chemical species within the instrument are essential given the broad application of these instruments in atmospheric observation networks.

In this work, $\text{RIE}_{\text{OA}}^{\text{*CE}}$, RIE_{OA} , RIE_{NH_4} , and Pieber artifacts were evaluated under controlled conditions of both particle concentration and composition for three pure organic compounds as well as mixtures of organic compounds with ammonium nitrate.

The measured $\text{RIE}_{\text{OA}}^{\text{*CE}}$ across multiple instruments under the same laboratory conditions for pure levoglucosan gives an average value of 1.78 ± 0.35 . Since this value is influenced by CE, which is related to particle phase and can vary across the sampling line, an RIE_{OA} independent of CE was calculated using binary organic-ammonium nitrate mixtures using nitrate as an internal reference. This work

illustrated that despite having average RIE values consistent with previous work, instrument-to-instrument variability occurs and can lead to significant variability (RIE ranging from 1 to 1.6) when performing such measurements using a single instrument.

Several methodologies were investigated to calculate RIE for both pure and mixed organic solutions, building on previous work. Having a large number of instruments, we demonstrated the range of instrument variability and compared results with previously reported values, enabling us to assess expected uncertainty ranges.

Another purpose of the study focused on the m/z 44 artifact. The variability of this artifact over a two-year period was assessed, (between the 2016 ACTRIS calibration workshop and the present one). A high degree of variability in the Pieber-type artifact values was observed between both campaigns. Of the five instruments participating in both intercomparisons, only one maintained a similar Pieber artifact over the years, while three instruments (Nos. 1, 3, 6) have increased m/z 44 signal in the presence of NO_3 fraction (m/z 44/ $\text{NO}_3 \geq 0.10$), and the fifth instrument no longer had an artifact. This variability in the Pieber artifact suggests the need for frequent evaluation and quantification that can be made during standard calibrations (recommended every 6 months). Testing the behavior of instruments for the Pieber artifact using the binary organic sugar-ammonium nitrate mixtures revealed that those instruments having artifacts at low NMF also had artifacts in the organic mixtures. However, these artifacts appeared at much lower NMF (<0.5) and are therefore more atmospherically relevant.

The current work illustrates that these artifacts occur across both inorganic and organic mixtures and assesses the presence of this artifact for each of the participating instruments. The impact of the Pieber artifact on the O:C ratio has not previously been demonstrated. Our findings illustrate that when Pieber artifacts fall in the range of 0.05 to 0.15, an application of a correction across all ammonium nitrate mass fractions (NMF) can result in an improved agreement of O:C ratios across instruments. However, for higher artifact values (>0.15), further investigations are required, as it was demonstrated by Freney et al. (2019) that correction for high artifact values across all NMF can result in an underestimation of f_{44} .

This study demonstrates that the presence of artifacts in three instruments does not affect source apportionment factor separation of primary and secondary organic species. However, it may influence the

interpretation of ambient measurement data and source apportionment analysis in polluted environments or during laboratory experiments with high NMF. The impact of this artifact in mixtures with less oxygenated organic compounds is unknown and should be further investigated.

Overall, these findings from laboratory and ambient air experiments provide valuable insights for the calibration and operation of ACSM instruments, and future studies can build on this work to further evaluate and improve instrument performances.

Acknowledgments

The authors gratefully acknowledge all the LSCE and Ineris personnel, as well as the support of INSU for the operation of both SI-SIRTA and SNO-CLAP of which the ACMCC belongs. L.M. acknowledges the support of Romanian National Core Program Contract No. 18N/2019, FORCLIMSOC Programme (Contract No. 12N/2023), Project IDs PN 23090101 the Romanian Ministry of Research, Innovation and Digitalization, through Program 1 – Development of the national research-development system, Subprogram 1.2 – Institutional performance – Projects to finance the excellent RDI, CresPerfInst project Contract No. 34PFE./30.12.2021 and Contract No. 18PFE/30.12.2021, and the European Regional Development Fund through the Competitiveness Operational Programme 2014–2020, POC-A.1-A.1.1.1-F-2015, project Research Centre for Environment and Earth Observation CEO-Terra, SMIS code 108109, Contract No. 152/2016.

Disclosure statement

No potential conflict of interest was reported by the author(s).

Funding

The work performed for this study was partially funded by COST Action “COLOSSAL” under grant agreement CA16109 and ACTRIS-2 H2020 research project under Grant agreement 654109. CNRS-INSU is also routinely supporting the various activities performed at the ACMCC included within the long-term monitoring aerosol program SNO-CLAP, both of which are components of the ACTRIS French Research Infrastructure.

ORCID

Luminița Mărmureanu  <http://orcid.org/0000-0001-8151-2304>

Leah Williams  <http://orcid.org/0000-0002-8505-9591>

Evelyn Freney  <http://orcid.org/0000-0002-9363-9115>

References

- Belis, C. A., F. Karagulian, B. R. Larsen, and P. K. Hopke. 2013. Critical review and meta-analysis of ambient particulate matter source apportionment using receptor models in Europe. *Atmos. Environ.* 69:94–108. doi: 10.1016/j.atmosenv.2012.11.009.
- Bressi, M., F. Cavalli, J. P. Putaud, R. Fröhlich, J.-E. Petit, W. Aas, M. Äijälä, A. Alastuey, J. D. Allan, M. Aurela, et al. 2021. A European aerosol phenomenology – 7: High-time resolution chemical characteristics of submicron particulate matter across Europe. *Atmos. Environ. X* 10:100108. doi: 10.1016/j.aeaoa.2021.100108.
- Budisulistiorini, S. H., M. R. Canagaratna, P. L. Croteau, K. Baumann, E. S. Edgerton, M. S. Kollman, N. L. Ng, V. Verma, S. L. Shaw, E. M. Knipping, et al. 2014. Intercomparison of an aerosol chemical speciation monitor (ACSM) with ambient fine aerosol measurements in downtown Atlanta, Georgia. *Atmos. Meas. Tech.* 7 (7): 1929–1941. doi: 10.5194/amt-7-1929-2014.
- Canagaratna, M., J. Jayne, J. Jimenez, J. Allan, M. Alfarra, Q. Zhang, T. Onasch, F. Drewnick, H. Coe, A. Middlebrook, et al. 2007. Chemical and microphysical characterization of ambient aerosols with the Aerodyne aerosol mass spectrometer. *Mass Spectrom. Rev.* 26 (2): 185–222. doi: 10.1002/mas.20115.
- Canagaratna, M. R., J. L. Jimenez, J. H. Kroll, Q. Chen, S. H. Kessler, P. Massoli, L. Hildebrandt Ruiz, E. Fortner, L. R. Williams, K. R. Wilson, et al. 2015. Elemental ratio measurements of organic compounds using aerosol mass spectrometry: Characterization, improved calibration, and implications. *Atmos. Chem. Phys.* 15 (1):253–272. doi: 10.5194/acp-15-253-2015.
- Canonaco, F., M. Crippa, J. G. Slowik, U. Baltensperger, and A. S. H. Prévôt. 2013. SoFi, an IGOR-based interface for the efficient use of the generalized multilinear engine (ME-2) for source apportionment: ME-2 application to aerosol mass spectrometer data. *Atmos. Meas. Tech.* 6 (12):3649–3661. doi: 10.5194/amt-6-3649-2013.
- Canonaco, F., A. Tobler, G. Chen, Y. Sosedova, J. G. Slowik, C. Bozzetti, K. R. Daellenbach, I. El Haddad, M. Crippa, R.-J. Huang, et al. 2021. A new method for long-term source apportionment with time-dependent factor profiles and uncertainty assessment using SoFi Pro: Application to 1 year of organic aerosol data. *Atmos. Meas. Tech.* 14 (2):923–943. doi: 10.5194/amt-14-923-2021.
- Chen, G., F. Canonaco, A. Tobler, W. Aas, A. Alastuey, J. Allan, S. Atabakhsh, M. Aurela, U. Baltensperger, A. Bougiatioti, et al. 2022. European aerosol phenomenology – 8: Harmonised source apportionment of organic aerosol using 22 year-long ACSM/AMS datasets. *Environ. Int.* 166:107325. doi: 10.1016/j.envint.2022.107325.
- Crenn, V., J. Sciare, P. L. Croteau, S. Verlhac, R. Fröhlich, C. A. Belis, W. Aas, M. Äijälä, A. Alastuey, B. Artigiani, et al. 2015. ACTRIS ACSM intercomparison - Part 1: Reproducibility of concentration and fragment results from 13 individual Quadrupole Aerosol Chemical Speciation Monitors (Q-ACSM) and consistency with co-located instruments. *Atmos. Meas. Tech.* 8 (12):5063–5087. doi: 10.5194/amt-8-5063-2015.

- Crippa, M., P. F. DeCarlo, J. G. Slowik, C. Mohr, M. F. Heringa, R. Chirico, L. Poulain, F. Freutel, J. Sciare, J. Cozic, et al. 2013. Wintertime aerosol chemical composition and source apportionment of the organic fraction in the metropolitan area of Paris. *Atmos. Chem. Phys.* 13 (2):961–981. doi: 10.5194/acp-13-961-2013.
- Daellenbach, K. R., G. Uzu, J. Jiang, L.-E. Cassagnes, Z. Leni, A. Vlachou, G. Stefanelli, F. Canonaco, S. Weber, A. Segers, et al. 2020. Sources of particulate-matter air pollution and its oxidative potential in Europe. *Nature* 587 (7834):414–419. doi: 10.1038/s41586-020-2902-8.
- Frenay, E., Y. Zhang, P. Croteau, T. Amodeo, L. Williams, F. Truong, J. Petit, J. Sciare, R. Sarda-Estève, N. Bonnaire, et al. 2019. The second ACTRIS intercomparison (2016) for Aerosol Chemical Speciation Monitors (ACSM): calibration protocols and instrument performance evaluations. *Aerosol Sci. Technol.* 53 (7):830–842. doi: 10.1080/02786826.2019.1608901.
- Fröhlich, R., V. Crenn, A. Setyan, C. A. Belis, F. Canonaco, O. Favez, V. Riffault, J. G. Slowik, W. Aas, M. Aijälä, et al. 2015. ACTRIS ACSM intercomparison – Part 2: Intercomparison of ME-2 organic source apportionment results from 15 individual, co-located aerosol mass spectrometers. *Atmos. Meas. Tech.* 8 (6):2555–2576. doi: 10.5194/amt-8-2555-2015.
- Huffman, J. A., J. Jayne, F. Drewnick, A. C. Aiken, T. Onasch, D. Worsnop, and J. Jimenez. 2005. Design, modeling, optimization, and experimental tests of a particle beam width probe for the Aerodyne Aerosol Mass Spectrometer. *Aerosol Sci. Technol.* 39 (12):1143–1163. doi: 10.1080/02786820500423782.
- IPCC. 2021. Summary for policymakers. In *Climate change 2021: The physical science basis. contribution of working group I to the sixth assessment report of the intergovernmental panel on climate change*, eds. V. Masson-Delmotte, P. Zhai, A. Pirani, S. L. Connors, C. Péan, S. Berger, N. Caud, Y. Chen, L. Goldfarb, M. I. Gomis, M. Huang, K. Leitzell, E. Lonnoy, J. B. R. Matthews, T. K. Maycock, T. Waterfield, O. Yelekçi, R. Yu and B. Zhou. <https://www.ipcc.ch/report/ar6/wg1/chapter/summary-for-policymakers/>.
- Jimenez, J. L., M. R. Canagaratna, F. Drewnick, J. D. Allan, M. R. Alfarra, A. M. Middlebrook, J. G. Slowik, Q. Zhang, H. Coe, J. T. Jayne, et al. 2016. Comment on ‘The effects of molecular weight and thermal decomposition on the sensitivity of a thermal desorption aerosol mass spectrometer. *Aerosol Sci. Technol.* 50 (9):i–xv. doi: 10.1080/02786826.2016.1205728.
- Jimenez, J. L., M. R. Canagaratna, N. M. Donahue, A. S. H. Prevot, Q. Zhang, J. H. Kroll, P. F. DeCarlo, J. D. Allan, H. Coe, N. L. Ng, et al. 2009. Evolution of organic aerosols in the atmosphere. *Science* 326 (5959):1525–1529. doi: 10.1126/science.1180353.
- Johannesson, S., P. Gustafson, P. Molnár, L. Barregard, and G. Sällsten. 2007. Exposure to fine particles (PM_{2.5} and PM₁) and black smoke in the general population: Personal, indoor, and outdoor levels. *J. Expo. Sci. Environ. Epidemiol.* 17 (7):613–624. doi: 10.1038/sj.jes.7500610.
- Karagulian, F., and C. Belis. 2012. Enhancing source apportionment with receptor models to foster the air quality directive implementation. *IJEP.* 50 (1/2/3/4):190–199. doi: 10.1504/IJEP.2012.051192.
- Kawamura, K., and S. Bikkina. 2016. A review of dicarboxylic acids and related compounds in atmospheric aerosols: Molecular distributions, sources, and transformation. *Atmos. Res.* 170:140–160. doi: 10.1016/j.atmosres.2015.11.018.
- Mărmureanu, L., J. Vasilescu, J. Slowik, A. S. H. Prévôt, C. A. Marin, B. Antonescu, A. Vlachou, A. Nemuc, A. Dandocsi, and S. Szidat. 2020. Online chemical characterization and source identification of summer and winter aerosols in Măgurele, Romania. *Atmosphere* 11 (4):385. doi: 10.3390/atmos11040385.
- Middlebrook, A. M., R. Bahreini, J. L. Jimenez, and M. R. Canagaratna. 2012. Evaluation of composition-dependent collection efficiencies for the Aerodyne aerosol mass spectrometer using field data. *Aerosol Sci. Technol.* 46 (3): 258–271. doi: 10.1080/02786826.2011.620041.
- Nault, B. A., P. Croteau, J. Jayne, A. Williams, L. Williams, D. Worsnop, E. F. Katz, P. F. DeCarlo, and M. Canagaratna. 2023. Laboratory evaluation of organic aerosol relative ionization efficiencies in the aerodyne aerosol mass spectrometer and aerosol chemical speciation monitor. *Aerosol Sci. Technol.* 57 (10):981–997. doi: 10.1080/02786826.2023.2223249.
- Ng, N. L., S. C. Herndon, A. Trimborn, M. R. Canagaratna, P. L. Croteau, T. B. Onasch, D. Sueper, D. R. Worsnop, Q. Zhang, Y. L. Sun, et al. 2011. An aerosol chemical speciation monitor (ACSM) for routine monitoring of the composition and mass concentrations of ambient aerosol. *Aerosol Sci. Technol.* 45 (7):780–794. doi: 10.1080/02786826.2011.560211.
- Paatero, P. 1999. The multilinear engine: A table-driven, least squares program for solving multilinear problems, including the n Way parallel factor analysis model. *J. Comput. Graph. Stat.* 8 (4):854. doi:10.2307/1390831.
- Petit, J.-E., O. Favez, J. Sciare, V. Crenn, R. Sarda-Estève, N. Bonnaire, G. Močnik, J.-C. Dupont, M. Haeffelin, and E. Leoz-Garziandia. 2015. Two years of near real-time chemical composition of submicron aerosols in the region of Paris using aerosol chemical speciation monitor (ACSM) and multi-wavelength aethalometer. *Atmos. Chem. Phys.* 15 (6):2985–3005. doi: 10.5194/acp-15-2985-2015.
- Pieber, S. M., I. El Haddad, J. G. Slowik, M. R. Canagaratna, J. T. Jayne, S. M. Platt, C. Bozzetti, K. R. Daellenbach, R. Fröhlich, A. Vlachou, et al. 2016. Inorganic salt interference on CO₂⁺ in Aerodyne AMS and ACSM organic aerosol composition studies. *Environ. Sci. Technol.* 50 (19):10494–10503. doi: 10.1021/acs.est.6b01035.
- Poulain, L., G. Spindler, A. Grüner, T. Tuch, B. Stieger, D. van Pinxteren, J.-E. Petit, O. Favez, H. Herrmann, and A. Wiedensohler. 2020. Multi-year ACSM measurements at the central European research station Melpitz (Germany) – Part 1: Instrument robustness, quality assurance, and impact of upper size cutoff diameter. *Atmos. Meas. Tech.* 13 (9):4973–4994. doi: 10.5194/amt-13-4973-2020.
- Tobler, A. K., A. Skiba, D. S. Wang, P. Croteau, K. Styszko, J. Nęcki, U. Baltensperger, J. G. Slowik, and A. S. H. Prévôt. 2020. Improved chloride quantification in quadrupole aerosol chemical speciation monitors (Q-ACSMs).

- Atmos. Meas. Tech.* 13 (10):5293–5301. doi: [10.5194/amt-13-5293-2020](https://doi.org/10.5194/amt-13-5293-2020).
- Viana, M., T. Kuhlbusch, X. Querol, A. Alastuey, R. Harrison, P. Hopke, W. Winiwarter, M. Vallius, S. Szidat, A. Prévôt, et al. 2008. Source apportionment of particulate matter in Europe: A review of methods and results. *J. Aerosol Sci.* 39 (10):827–849. doi: [10.1016/j.jaerosci.2008.05.007](https://doi.org/10.1016/j.jaerosci.2008.05.007).
- Xu, W., A. Lambe, P. Silva, W. Hu, T. Onasch, L. Williams, P. Croteau, X. Zhang, L. Renbaum-Wolff, E. Fortner, et al. 2018. Laboratory evaluation of species-dependent relative ionization efficiencies in the Aerodyne aerosol mass spectrometer. *Aerosol Sci. Technol.* 52 (6):626–641. doi: [10.1080/02786826.2018.1439570](https://doi.org/10.1080/02786826.2018.1439570).
- Zhang, Q., J. L. Jimenez, M. R. Canagaratna, J. D. Allan, H. Coe, I. Ulbrich, M. R. Alfarra, A. Takami, A. M. Middlebrook, Y. L. Sun, et al. 2007. Ubiquity and dominance of oxygenated species in organic aerosols in anthropogenically-influenced Northern Hemisphere mid-latitudes. *Geophys. Res. Lett.* 34 (13):801. doi: [10.1029/2007GL029979](https://doi.org/10.1029/2007GL029979).
- Zhang, Y., L. Tang, P. L. Croteau, O. Favez, Y. Sun, M. R. Canagaratna, Z. Wang, F. Couvidat, A. Albinet, H. Zhang, et al. 2017. Field characterization of the PM_{2.5} Aerosol Chemical Speciation Monitor: Insights into the composition, sources, and processes of fine particles in eastern China. *Atmos. Chem. Phys.* 17 (23):14501–14517. doi: [10.5194/acp-17-14501-2017](https://doi.org/10.5194/acp-17-14501-2017).
- Zhang, Y., O. Favez, J.-E. Petit, F. Canonaco, F. Truong, N. Bonnaire, V. Cretnn, T. Amodeo, A. S. H. Prévôt, J. Sciare, et al. 2019. Six-year source apportionment of sub-micron organic aerosols from near-continuous highly time-resolved measurements at SIRTa (Paris area, France). *Atmos. Chem. Phys.* 19 (23):14755–14776. doi: [10.5194/acp-19-14755-2019](https://doi.org/10.5194/acp-19-14755-2019).